arXiv:1209.6436v1 [cond-mat.str-el] 28 Sep 2012

Frustration induced spin glass behaviour in $Ba_3RuTi_2O_9$

Tusharkanti Dey* and A.V. Mahajan
Department of Physics, Indian Institute of Technology Bombay, Powai, Mumbai 400076, India

Abstract

Hexagonal $Ba_3RuTi_2O_9$ consists of a layered triangular network of $Ru^{4+}(S = 1)$ ions. Magnetic susceptibility $\chi(T)$ and heat capacity data show no long range magnetic ordering down to 1.8 K. A Curie-Weiss (CW) fitting of $\chi(T)$ yields a large antiferromagnetic CW temperature $\theta_{\rm CW} = -166$ K. However, with low field, a splitting of zero field cooled (ZFC) and field cooled (FC) $\chi(T)$ is observed below $\sim$ 30K. Our measurements suggest that $Ba_3RuTi_2O_9$ is a highly frustrated system and some parts of the material undergo a spin glass transition at 30 K.

PACS numbers: 75.47.Lx, 75.50.Lk, 75.40.Cx

I. INTRODUCTION

In recent times, 4*d* and 5*d* transition metal based materials have been in the focus as their driving physics is different from their 3*d* counterparts but have not been explored much. This variation arises because of their extended '*d*' orbitals, a small onsite Coulomb energy 'U', and a large spin-orbit coupling (SOC) [1]. The interplay between U and SOC makes these materials interesting. Many systems of the 4*d*/5*d* family like Sr_2(Ir/Ru/Rh)O_4 [1–3], Ca_2RuO_4 [4], Na_2IrO_3 [5], $Na_4Ir_3O_8$ [6], (Sr/Ca)$_3Ru_2O_7$ [7, 8] etc. have drawn attention in recent years.

Recently, we reported results of our investigations of hexagonal $Ba_3IrTi_2O_9$ with 5*d* Ir^{4+} ($J_{eff} = 1/2$) ions forming a 2D triangular network [9]. A large site-disorder between Ir^{4+} and Ti^{4+} cations plays an important role in the magnetic properties of the sample. The system remains paramagnetic down to 0.35 K despite a large antiferromagnetic (AF) Curie-Weiss temperature $\theta_{\rm CW} \sim -130$ K. Magnetic heat capacity at low temperature follows a power law with temperature. These results suggest that $Ba_3IrTi_2O_9$ is in a spin liquid ground state with 5*d* Ir^{4+} ($J_{eff} = 1/2$) in a 2D triangular network. The SOC presumably plays a significant role in determining the properties of the system. It will be interesting to study its 4*d*-analog (say, based on Ru) where spin-orbit coupling effect is expected to be of intermediate strength compared to that in 3*d* and 5*d* elements.

Dickson *et al.* [10] measured the magnetic susceptibility variation with temperature of hexagonal $Ba_3RuTi_2O_9$ in the limited temperature range 253 K to 323 K. Susceptibility data in a larger temperature range $77-335$ K are reported in Ref. [11]. In both the papers a high, AF $\theta_{\rm CW}$ (~ -250 K) is inferred [10, 11]. These reports indicate that $Ba_3RuTi_2O_9$ could also be a frustrated spin liquid candidate and a 4*d* analog of $Ba_3IrTi_2O_9$ with $S = 1$. Thus low temperature measurements on $Ba_3RuTi_2O_9$ are warranted to confirm its magnetic ground state.

In this paper we report preparation, structural analysis, magnetic susceptibility and heat capacity measurements on $Ba_3RuTi_2O_9$. The system crystallizes in the space group P6$_3$mc with a large site sharing between Ru^{4+} and Ti^{4+} ions as reported earlier [12] and similar to that in $Ba_3IrTi_2O_9$ [9]. Susceptibility data show no long range ordering down to 2K but splitting between zero field cooled (ZFC) and field cooled (FC) data is found below 30 K. A large $\theta_{\rm CW}$ (AF) obtained from CW fitting indicates strong correlation between the magnetic ions. No anomaly, even at 30 K, is found in heat capacity measurements down to 1.8 K. These measurements suggest that the system is highly frustrated and perhaps a fraction of the spins participate in a spin glass state below 30 K.

II. EXPERIMENTAL DETAILS

A polycrystalline sample of $Ba_3RuTi_2O_9$ was prepared by conventional solid state reaction method using high purity $BaCO_3$, TiO_2 and Ru metal powder as starting materials. Stoichiometric amount of the starting materials were mixed thoroughly, pressed into a pellet and calcined at 900^0C for 15 h. After calcination, the pellet was crushed into powder, pelletized and fired at 1100^0C for 100 h with several intermediate grindings.

Powder x-ray diffraction (XRD) measurements were performed at room temperature with Cu K_α radiation ($\lambda = 1.54182$Å) in a PANalytical X'Pert PRO diffractometer using Si for calibration. Magnetization M measurements were carried out in the temperature T range $2-400$ K using Quantum Design PPMS and SQUID VSM. Heat capacity measurements were done in the temperature range $1.8-300$ K and field H range $0-9$ T using the heat capacity attachment of Quantum Design PPMS.

III. RESULTS AND DISCUSSIONS

Single phase nature of our sample was confirmed from the XRD measurements. Maunders *et al.* have reported $Ba_3RuTi_2O_9$ to crystallize in the space group P6$_3$*mc* [13]. In this space group, the 2a site is occupied by the Ti^{4+} ions and in the 2b sites Ti^{4+}/Ru^{4+} ions reside in an or-

---

*Email: tusdey@gmail.com

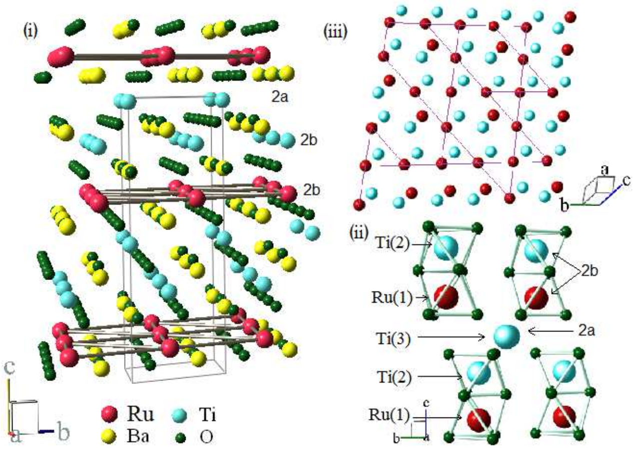

Figure 1: (i) Ideal structure of $Ba_3RuTi_2O_9$ without any site disorder between Ti^{4+} and Ru^{4+} ions. The Ru^{4+} spins form an edge shared triangular network parallel to the *ab* plane as shown. (ii) $RuTiO_9$ bioctahedra are shown (iii) A possible arrangement of Ti^{4+} and Ru^{4+} ions in the *ab* plane is shown when about 33% of Ru^{4+} ions exchange site with Ti^{4+} ions in the 2b site.

Table I: Lattice constants of $Ba_3RuTi_2O_9$ obtained from refinement and comparison with others.

Material	Space group	a (Å)	c (Å)	Source
$Ba_3RuTi_2O_9$	$P6_3mc$	5.7204	14.0109	this work
$Ba_3RuTi_2O_9$	$P6_3mc$	5.7056	14.0093	Ref. [13]
$Ba_3IrTi_2O_9$	$P6_3mc$	5.7214	14.0721	Ref. [9]
$BaTiO_3$	$P6_3/mmc$	5.7238	13.9649	Ref. [14]

Table II: Atomic parameters obtained by refining x-ray powder diffraction data for $Ba_3RuTi_2O_9$ at room temperature with the space group $P6_3mc$.

		x	y	z	g
Ba(1)	2a	0	0	0.249	1.00
Ba(2)	2b	1/3	2/3	0.085	1.00
Ba(3)	2b	1/3	2/3	0.397	1.00
Ru(1)	2b	1/3	2/3	0.65	0.61
Ti(1)	2b	1/3	2/3	0.65	0.39
Ti(2)	2b	1/3	2/3	0.839	0.69
Ru(2)	2b	1/3	2/3	0.839	0.31
Ti(3)	2a	0	0	0.510	0.92
Ru(3)	2a	0	0	0.510	0.08
O(1)	6c	0.16098	0.83898	0.57538	1.00
O(2)	6c	0.48859	0.51138	0.74989	1.00
O(3)	6c	0.16098	0.83898	0.91548	1.00

dered manner. In the ideal case, the ordered arrangement of Ti^{4+} and Ru^{4+} ions form face-sharing $RuTiO_9$ bioctahedra (Fig. 1(ii)) and the Ru^{4+} spins form an edge-shared triangular network in the *ab* plane (as shown in Fig. 1(i)). However, a site sharing between Ti^{4+} and Ru^{4+} ions is expected as the two ions are of similar ionic size. In Ref. [12] four possible arrangements of Ru^{4+}/Ti^{4+} ions have been suggested in $Ba_3RuTi_2O_9$. Among them two are most probable where $RuTiO_9$ and Ru_2O_9/Ti_2O_9 bioctahedra are formed. We refined of our XRD data using the space group $P6_3mc$ and considering a site sharing between Ti^{4+} and Ru^{4+} ions. We have found almost 31% site exchange of Ru^{4+} ions with Ti^{4+} ions in the 2b site and an 8% site sharing with 2a site Ti^{4+} ions. This situation is very similar to that found in Ref. [12]. In $Ba_3IrTi_2O_9$ as well, we found a large site sharing of Ir^{4+} ions with Ti^{4+} ions both in 2b as well as 2a sites [9].

Fig. 2 shows the XRD refinement pattern which yields R_p = 5.7%, R_{wp} = 7.7% and goodness of fit (GOF)= 9.700. The lattice parameters obtained from the refinement are shown in Table I and compared with the values with $Ba_3RuTi_2O_9$ (reported earlier), $Ba_3IrTi_2O_9$ and $BaTiO_3$ (parent compound). Values obtained by us are in good agreement with others. The atomic positions and occupancies resulting from our refinement are shown in Table II.

As a result of site sharing between Ti^{4+} and Ru^{4+} ions, the Ru^{4+} ($S = 1$) edge shared triangular plane will be highly depleted. A probable situation is shown in Fig. 1(iii) where many of the misplaced Ru^{4+} ions can still manage to interact with other Ru^{4+} ions forming clusters, while some, called orphan spins, remain isolated.

Further we have measured susceptibility of the material at different fields as shown in Fig. 3. No long range magnetic ordering down to 2 K is found whereas a splitting between ZFC and FC data at 30 K is seen which may be indicative of a transition to a glassy state. The splitting is large, which indicates that a reasonable fraction of the spins are participating in the glassy phase. With increasing field, the splitting becomes less prominent and vanishes at an applied field of 10 kOe.

We have fitted susceptibility data with CW formula $\chi = \chi_0 + C/(T-\theta)$ in the temperature range $100-350$ K (shown in Fig 4) which yields the temperature independent susceptibility $\chi_0 = 2.05\times10^{-4}\,\mathrm{cm^3/mol}$, Curie constant $C = 0.7\,\mathrm{cm^3K/mol}$ and $\theta_{\mathrm{CW}} = -166$ K. For insulating oxides one can consider $\chi_0 = \chi_{core} + \chi_{vv}$, where χ_{core} is the core diamagnetic susceptibility and χ_{vv} is Van-Vleck paramagnetic susceptibility. For our sample $\chi_{core} = -2.32\times10^{-4}\,\mathrm{cm^3/mol}$ [15], which results in $\chi_{vv} = 4.37\times10^{-4}\,\mathrm{cm^3/mol}$. This value of χ_{vv} is similar to that found in other Ru based insulating oxides like La_2RuO_5 [16], La_2LiRuO_6 [17] etc. Inverse susceptibility is shown on the right axis of Fig. 4 (after subtracting the temperature independent part χ_0) which is linear with temperature in a wide range of temperature and deviates from linearity below ~ 80 K.

We now compare our susceptibility data with that of Ref. [11] by Bryne *et al.* A slope change was found by Bryne *et al.* in the inverse susceptibility of $Ba_3RuTi_2O_9$ at 150 K which is absent in our data. Moreover, they

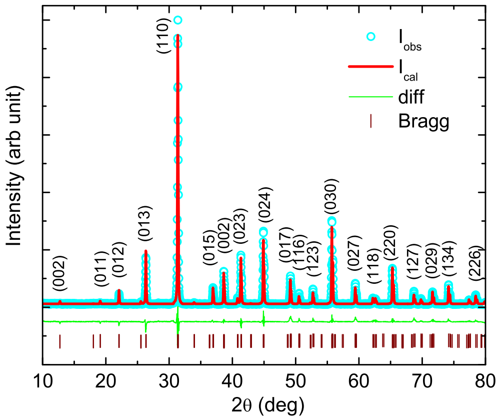

Figure 2: Refinement pattern of $Ba_3RuTi_2O_9$ with space group P6_3mc. Light blue circles indicate experimental pattern and the red line indicate the theoretical pattern while the green line is the difference between the two. The Bragg positions are shown as vertical lines. The (hkl) planes corresponding to the peaks are also marked in the figure.

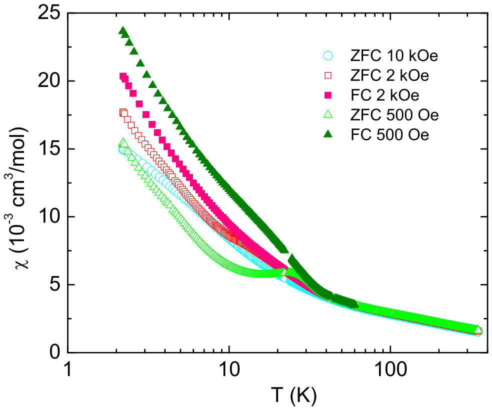

Figure 3: Magnetic susceptibility of $Ba_3RuTi_2O_9$ at different fields is shown as a function of temperature in semi-log scale. Solid symbols represent FC and open symbols represent ZFC measurements.

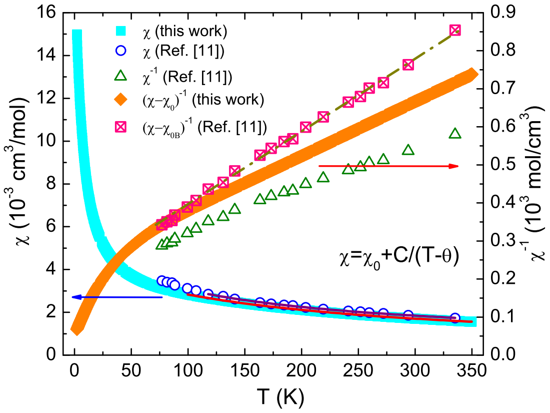

Figure 4: Magnetic susceptibility of $Ba_3RuTi_2O_9$ and its fitting with the Curie-Weiss law (red solid line). Inverse susceptibility (after subtracting χ_0) is shown as orange diamonds. Inverse susceptibility data of $Ba_3RuTi_2O_9$ obtained from Ref. [11] is shown as green triangles. The corresponding susceptibility is shown as blue circles with its fit with CW law (violet solid line). Inverse susceptibility after subtracting $\chi_{0\mathrm{B}}$ (obtained from fit) is also shown as pink squares. The dashed line is a guide to eye. All susceptibilities are plotted on the left axis while inverse susceptibilities correspond to the right axis. The solid symbols denote the data from this work and open symbols are used for data from Ref. [11].

found $\theta_{\mathrm{CW}} = -256\,\mathrm{K}$ and $\mu_{eff} = 2.86\mu_B$ which are higher than $\theta_{\mathrm{CW}} = -166\,\mathrm{K}$ and $\mu_{eff} = 2.37\mu_B$ obtained from our analysis. To clarify this discrepancy, we have reanalysed the published data as shown in Fig. 4. The green triangles represent the inverse susceptibility data as published in Ref. [11]. Corresponding susceptibility is shown as blue circles on the left axis and fitted by us with the CW law in the range $118 - 335\,\mathrm{K}$. This fitting gives $\chi_{0\mathrm{B}} = 5.55 \times 10^{-4}\,\mathrm{cm}^3/\mathrm{mol}$, $C = 0.54\,\mathrm{cm}^3\mathrm{K/mol}$ ($\mu_{eff} = 2.08\mu_B$) and $\theta_{\mathrm{CW}} = -116\,\mathrm{K}$. These values are somewhat closer to the values obtained by us. Subtracting this $\chi_{0\mathrm{B}}$, we have plotted $(\chi - \chi_{0\mathrm{B}})^{-1}$ which is linear in the whole temperature range and the kink at 150 K is also absent. Apparently, Bryne *et al.* did not use the correct χ_0 leading them to infer an incorrect Curie term. Also, they calculated μ_{eff} based on a single susceptibility data point (one temperature) which certainly can mislead.

The C value obtained from CW fit of our data is almost 70% of the paramagnetic $S = 1$ value. Normally in 3d transition metal oxides the C value turns out as expected from a pure spin contribution. But for 5d transition metal oxides the C value obtained is normally much smaller than expected from a pure spin contribution. In case of $Ba_3IrTi_2O_9$ this was only 40% of the expected spin-only value [9]. For 4d based systems the orbital effect is expected to be in between 3d and 5d materials. Hence the reduction in C obtained from our analysis is most likely an effect of spin-orbit coupling present in the system. A high ($-166\,\mathrm{K}$) θ_{CW} obtained from CW fit confirms that the Ru^{4+} spins are strongly correlated. Probably a large site sharing is responsible in forming magnetic clusters which give rise to the glassy behavior below 30K.

Heat capacity (C_{P}) of a material gives prominent signatures pertaining to any structural or magnetic transitions. We have measured C_{P} at different fields as shown in Fig. 5. Surprisingly, no anomaly, even at 30 K is found in C_{P} measurements. In the low temperature region, C_{P} depends on applied field which can be seen clearly in the inset of Fig. 5 showing C_{P}/T as a function of T.

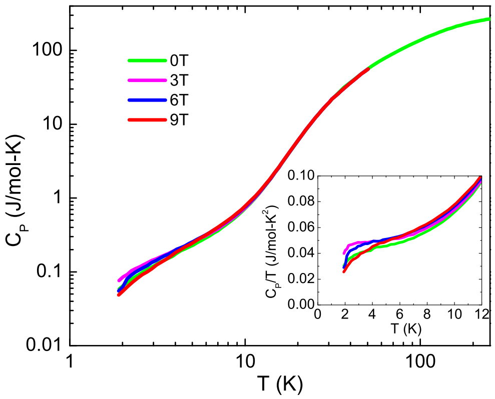

Figure 5: Heat capacity of $Ba_3RuTi_2O_9$ measured at different fields is shown in a log-log scale. Inset: C_P/T is shown as a function of T in the low-T region.

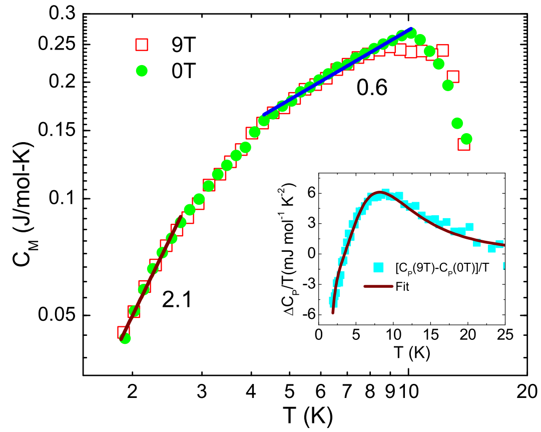

Figure 6: Magnetic heat capacity of $Ba_3RuTi_2O_9$ at 0T and 9T are shown in a log-log scale. The solid lines shows power law with temperature with the power shown in figure. Inset: $[C_P$ (9T)- C_P (0T)$]/T$ and its fit with Schottky model (solid line) is shown.

This field dependence could be arising from a Schottky anomaly of orphan spins present in the sample. The absence of an anomaly at the spin glass transition temperature (30 K) could be due to a large contribution from the crystal part supressing a small magnetic part at such high temperature. In this context we should mention that no anomaly in heat capacity is found in case of $Ba_3IrTi_2O_9$ [9] and $Ba_3TiIr_2O_9$ [18] where ZFC and FC susceptibilities split up at 80 K and 60 K, respectively. Also, it is possible that only a fraction of the spins are involved in the glassy phase while the rest are not, similar to $Ba_3IrTi_2O_9$ [9].

The total heat capacity of the sample has three contributions namely, (i) lattice contribution ($C_{\rm lat}$) (ii) magnetic contribution ($C_{\rm M}$) and (iii) Schottky contribution ($C_{\rm Sch}$) from orphan spins. The nuclear Schottky anomaly normally appears at much lower temperature and probably will not affect our data which is down to 1.8 K only. To extract the magnetic heat capacity we have to subtract out the $C_{\rm lat}$ and $C_{\rm Sch}$ from the total heat capacity. We now attempt to estimate the magnetic contribution by subtracting the other two parts.

The generalised heat capacity expression for two level Schottky anomaly is [19, 20],

$$C_{\rm Sch}(\Delta) = R\frac{g_0}{g_1}\left(\frac{\Delta}{k_BT}\right)^2 \frac{exp\left(\frac{\Delta}{k_BT}\right)}{\left[1+\frac{g_0}{g_1}exp\left(\frac{\Delta}{k_BT}\right)\right]^2} \qquad (1)$$

where Δ is the level splitting, R is the universal gas constant, k_B is the Boltzman constant and g_0 and g_1 are the degeneracies of ground state and excited state, respectively. For spin $S = 1$ (Ru^{4+}) systems, Eq. 1 can be modified with the approximation as $g_0 = 1$ and $g_1 = 2$ [19].

We have subtracted C_P(0T) from C_P(9T) data and further divided that by temperature. Any lattice contribution is therefore removed by this procedure. The $[C_P$(9T)-C_P(0T)$]/T$ data are shown in the inset of Fig. 6 with its fit to $f[C_{\rm Sch}(\Delta_{\rm 9T}) - C_{\rm Sch}(\Delta_{\rm 0T})]/T$. In this expression, f is the percentage of orphan spins present in the sample and $C_{\rm Sch}(\Delta_{\rm 9T})$, and $C_{\rm Sch}(\Delta_{\rm 0T})$ are the Schottky anomalies corresponding to the level splittings of $\Delta_{\rm 9T}$ and $\Delta_{\rm 0T}$ with applied magnetic fields 9T and 0T, respectively. The fit is reasonably good and suggests that the field dependence of C_P is coming from $C_{\rm Sch}$ only. From the fit we found $\Delta_{\rm 9T}/k_B = 27.7$ K, $\Delta_{\rm 0T}/k_B = 1.5$ K and $\sim 1\%$ orphan spins are present in the system. Putting the corresponding Δ (obtained from fitting) in Eq. 1 and multiplying by f, we can get the Schottky contribution ($C_{\rm Sch}$) to the heat capacity for a particular field.

To subtract the lattice contribution ($C_{\rm lat}$) from the total heat capacity (C_P) one needs a non-magnetic analog of the system. Unfortunately, we didn't find a good non-magnetic analog of $Ba_3RuTi_2O_9$. However we have earlier used $Ba_3ZnSb_2O_9$ (taken from Ref. [21]) as a non-magnetic analog in the case of $Ba_3IrTi_2O_9$ [9]. $Ba_3ZnSb_2O_9$ can be used as a non magnetic analog in the present case as well since both have similar crystal structure. The heat capacities of these two samples have a mismatch at higher temperature due to the difference in their molecular mass and volume. We have used a multification factor of ~ 0.67 so that C_P data of $Ba_3ZnSb_2O_9$ matches with that of $Ba_3RuTi_2O_9$ in the nominal temperature range $40 - 60$K. The corrected heat capacity of $Ba_3ZnSb_2O_9$ can be considered as the lattice contribution ($C_{\rm lat}$) to the total heat capacity of $Ba_3RuTi_2O_9$. This $C_{\rm lat}$ is subtracted from C_P and we are left with the $C_{\rm M}$ and $C_{\rm Sch}$. Further we have subtracted $C_{\rm Sch}$ obtained from our previous analysis and finally obtained $C_{\rm M}$.

The $C_{\rm M}$ is independent of field as shown in Fig. 6

and follows a power law in temperature with power 0.6 in the range $4.3-10\,\mathrm{K}$ and with power 2.1 below 2.7 K. This suggests that spin excitations are present in this system. We have also estimated the entropy change $\triangle \mathrm{S_M}$=0.36 J/mol-K by integrating C_{M}/T. This value is much smaller then expected value of 9.13 J/mol-K. This reduction could be partly due to a strong spin-orbit coupling present in the system. Most likely other reasons like error in estimation of C_{lat} due to lack of a proper non-magnetic analog are also responsible.

IV. CONCLUSIONS

We have prepared $\mathrm{Ba_3RuTi_2O_9}$ (a $4d$ analog of the $5d$ system $\mathrm{Ba_3IrTi_2O_9}$) and measured its magnetic susceptibility and heat capacity at different fields. No long range magnetic ordering is found down to 1.8 K despite a large θ_{CW} obtained from CW fitting of susceptibility data. This indicates that the spins are strongly correlated and the system is highly frustrated. Magnetic moments are reduced probably because of a spin-orbit coupling present in this system. Splitting of ZFC and FC susceptibility data at 30 K indicates formation of a glassy phase. However, absence of an heat capacity anomaly at this temperature probably suggests that a fraction of the spins participate in this glassy phase. Magnetic heat capacity of this material is independent of field and approaches a power law at low temperature with power 2.1. These measurements suggest that $\mathrm{Ba_3RuTi_2O_9}$ is a highly frustrated system but the nature of its ground state is not very clear. Local probe investigations like μSR could be useful to check if the spin freezing happens in the bulk of the sample or not.

V. ACKNOWLEDGEMENT

We thank Department of Science and Technology, Govt. of India for financial support.

---

[1] B. J. Kim, H. Jin, S. J. Moon, J.-Y. Kim, B.-G. Park, C. S. Leem, Jaejun Yu, T.W. Noh, C. Kim, S.-J. Oh, J.-H. Park, V. Durairaj, G. Cao, and E. Rotenberg, Phys. Rev. Lett. **101**, 076402 (2008)
[2] B. J. Kim, H. Ohsumi, T. Komesu, S. Sakai, T. Morita, H. Takagi, and T. Arima, Science **323**, 1329 (2009)
[3] M. W. Haverkort, I. S. Elfimov, L. H. Tjeng, G. A. Sawatzky, and A. Damascelli, Phys. Rev. Lett. **101**, 026406 (2008)
[4] T. Mizokawa, L. H. Tjeng, G. A. Sawatzky, G. Ghiringhelli, O. Tjernberg, N. B. Brookes, H. Fukazawa, S. Nakatsuji, and Y. Maeno, Phys. Rev. Lett. **87**, 077202 (2001)
[5] Y. Singh and P. Gegenwart, Phys. Rev. B **82**, 064412 (2010)
[6] Y. Okamoto, M. Nohara, H. Aruga-Katori, and H. Takagi, Phys. Rev. Lett. **99**, 137207 (2007)
[7] R. S. Perry, L. M. Galvin, S. A. Grigera, L. Capogna, A. J. Schofield, A. P. Mackenzie, M. Chiao, S. R. Julian, S. Ikeda, S. Nakatsuji, Y. Maeno, and C. Pfleiderer, Phys. Rev. Lett. **86**, 2661 (2001)
[8] G. Cao, X. N. Lin, L. Balicas, S. Chikara, J. E. Crow, and P. Schlottmann, New J. Phys. **6**, 159 (2004).
[9] T. Dey, A. V. Mahajan, P. Khuntia, M. Baenitz, B. Koteswararao, and F. C. Chou (unpublished)
[10] J. G. Dickson, L. Katz, and R. Ward, J. Amer. Chem. Soc. **83**, 3026 (1961)
[11] R. C. Byrne, and C. W. Moeller, J. Solid State Chem. **2**, 228 (1970)
[12] G. Radtke, C. Maunders, A. Saúl, S. Lazar, H. J. Whitfield, J. Etheridge, and G. A. Botton, Phys. Rev. B **81**, 085112 (2010)
[13] C. Maunders, J. Etheridge, N. Wright, and H. J. Whitfield, Acta Crystallogr., Sect. B: Struct. Sci. **61**, 154 (2005)
[14] J. Akimoto, Y. Gotoh, and Y. Oosawa, Acta Cryst. C **50**, 160 (1994)
[15] P. W. Selwood, Magnetochemistry (Interscience, New York, 1956)
[16] S. Riegg, A. Günther, H.-A. K. von Nidda, A. Loidl, M. V. Eremin, A. Reller, and S. G. Ebbinghaus, Phys. Rev. B **86**, 115125 (2012)
[17] T. Aharen, J. E. Greedan, F. Ning, T. Imai, V. Michaelis, S. Kroeker, H. Zhou, C. R. Wiebe, and L. M. D. Cranswick, Phys. Rev. B **80**, 134423 (2009)
[18] T. Sakamoto, Y. Doi, and Y. Hinatsu, J. Solid State Chem. **179**, 2595 (2006)
[19] E. S. R. Gopal, Specific Heats at Low Temperatures Plenum, New York, 1966
[20] C. He, H. Zheng, J. F. Mitchell, M. L. Foo, R. J. Cava, and C. Leighton, Appl. Phys. Lett. **94**, 102514 (2009)
[21] H. D. Zhou, E. S. Choi, G. Li, L. Balicas, C. R. Wiebe, Y. Qiu, J. R. D. Copley, and J. S. Gardner, Phys. Rev. Lett. **106**, 147204 (2011) and Supplemental Material of J. G. Cheng, G. Li, L. Balicas, J. S. Zhou, J. B. Goodenough, C. Xu, and H. D. Zhou, Phys. Rev. Lett. **107**, 197204 (2011)